

# Mono- and Binuclear Ruthenium Corroles: Synthesis, Spectroscopy, Electrochemistry, and Structural Characterization

Liliya Simkhovich,<sup>[a]</sup> Inna Luobeznova,<sup>[a]</sup> Israel Goldberg,<sup>\*[b]</sup> and Zeev Gross<sup>\*[a]</sup>

**Abstract:** The aim of this research was to prepare mononuclear ruthenium corroles, because of the well-documented potency of analogous porphyrin complexes in catalysis. The syntheses of the mononuclear nitrosyl complexes [Ru(tpfc)(NO)] and [Ru(tdcc)(NO)] (tpfc = trianion of 5,10,15-tris(pentafluorophenyl)corrole, tdcc = trianion of 5,10,15-tris(2,6-dichlorophenyl)corrole), and of the binuclear  $[[\text{Ru}(\text{tpfc})]_2]$  were achieved by using  $[[\text{Ru}(\text{cod})\text{Cl}_2]_x]$  (cod = cyclooctadiene) as the metal

source. The NMR spectra of all three complexes clearly demonstrate that they are diamagnetic; this is consistent with a triple bond between the metal ions in  $[[\text{Ru}(\text{tpfc})]_2]$  and is expected for classical {MNO}<sup>6</sup> complexes. These features were further substantiated by the stretching

**Keywords:** cyclic voltammetry · iron · NMR spectroscopy · porphyrinoids · ruthenium · X-ray diffraction

frequencies of the {MNO} moieties, electrochemical measurements on all complexes, and the X-ray crystal structures of [Ru(tpfc)(NO)] and  $[[\text{Ru}(\text{tpfc})]_2]$ . A comparison of the spectroscopic and structural characteristics of these new complexes with analogous iron corroles, as well as with iron and ruthenium porphyrins, suggests that it will be hard to obtain mononuclear ruthenium corroles without  $\pi$ -accepting ligands.

## Introduction

There has been a remarkable increase in research into corroles in the last three years.<sup>[1–18]</sup> This has been made possible by the introduction of three facile methodologies for their synthesis: the solvent-free condensation of pyrrole and aldehydes,<sup>[1]</sup> the modified Rothmund procedure,<sup>[2]</sup> and the dipyrromethane condensation with aldehydes.<sup>[3, 4]</sup> The revolution that these synthetic procedures initiated may be appreciated by the fact that while only three corroles substituted at the three *meso*-positions of the macrocycle were known prior to 1999,<sup>[5]</sup> the current number of such derivatives approaches 100. Among all these corroles, the *meso*-pentafluorophenyl derivative H<sub>3</sub>(tpfc) (tpfc = trianion of 5,10,15-tris(pentafluorophenyl)corrole) is by far the most intensively studied. This single corrole and its derivatives have been shown to support a large variety of metal ions (Cr,<sup>[6]</sup>

Mn,<sup>[7]</sup> Fe,<sup>[8]</sup> Co,<sup>[8a, 9]</sup> Rh,<sup>[8a, b, 10]</sup> Ni,<sup>[11]</sup> Pd,<sup>[11]</sup> Cu,<sup>[11]</sup> Zn,<sup>[12]</sup> Al,<sup>[13]</sup> Ga,<sup>[14]</sup> Ge,<sup>[8b]</sup> Sn,<sup>[8b]</sup> and P<sup>[8b]</sup>) and many of the complexes have been fully characterized in several oxidation and coordination states. Novel features of H<sub>3</sub>(tpfc) and its metal complexes include very high fluorescence quantum yield,<sup>[13, 14]</sup> easily achieved chirality,<sup>[10, 12]</sup> potent catalytic activity,<sup>[7a, c, 8b, 15]</sup> facile methodologies for further functionalization,<sup>[7c, 9, 10, 12, 16]</sup> and selective interactions with tumor cells.<sup>[17]</sup> Another important development is the introduction of corroles with *meso*-aryls that contain large *ortho*-phenyl substituents (Cl, CH<sub>3</sub>).<sup>[1a, 3c, d, f]</sup> These derivatives have been demonstrated to affect catalysis by avoiding the formation of binuclear  $\mu$ -oxo-bridged corroles.<sup>[8b]</sup>

Ruthenium is one of the most important metals in catalysis,<sup>[19]</sup> including porphyrin-based catalysts.<sup>[20]</sup> Accordingly, this was one of the first metals that we tried to insert into H<sub>3</sub>(tpfc). However, all our attempts to achieve the insertion with [Ru<sub>3</sub>(CO)<sub>15</sub>] and [Ru<sub>2</sub>Cl<sub>2</sub>(CO)<sub>6</sub>], which are the metal precursors that are used for ruthenium porphyrins, failed. Meanwhile, Guilard and co-workers reported the isolation of a bis-ruthenium corrole complex with  $[[\text{Ru}(\text{cod})\text{Cl}_2]_2]$  (cod = cyclooctadiene) as the metal source.<sup>[18]</sup> Taking advantage of these findings, we report here the syntheses of the binuclear  $[[\text{Ru}(\text{tpfc})]_2]$  and two novel mononuclear nitrosyl complexes, [Ru(tpfc)(NO)] and [Ru(tdcc)(NO)] (tdcc = trianion of 5,10,15-tris(2,6-dichlorophenyl)corrole) from this metal source. In addition to the synthetic aspects and several interesting spectroscopic features, we also present the rich electrochemistry of all three complexes and the high-resolution X-ray structures of  $[[\text{Ru}(\text{tpfc})]_2]$  and [Ru(tpfc)(NO)].

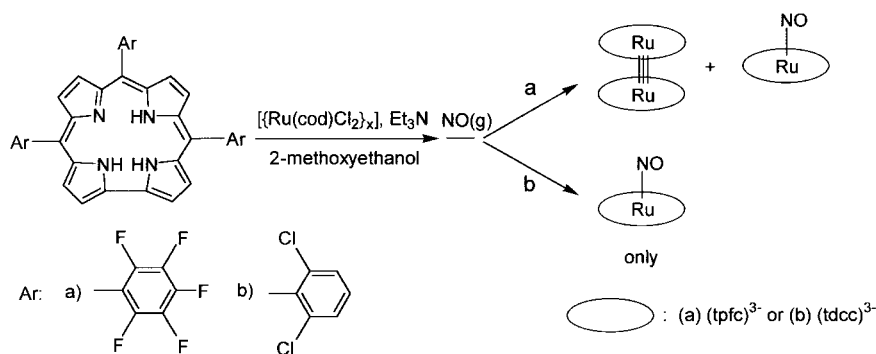
[a] Prof. Dr. Z. Gross, Dr. L. Simkhovich, I. Luobeznova  
Department of Chemistry and  
Institute of Catalysis Science and Technology  
Technion—Israel Institute of Technology  
Haifa 32000 (Israel)  
Fax: (+972)48-233-735  
E-mail: chr10zg@tx.technion.ac.il

[b] Prof. Dr. I. Goldberg  
School of Chemistry  
Tel Aviv University  
Tel Aviv 69978 (Israel)  
Fax: (+972)36-409-293  
E-mail: goldberg@chemsg7.tau.ac.il

## Results and Discussion

**Synthesis:** A major goal of these studies was the preparation of mononuclear corroles, because of the well-documented potency of ruthenium porphyrins in catalysis.<sup>[21]</sup> While these processes traditionally rely on ruthenium(II)/ruthenium(IV)/ruthenium(VI) oxidation states,<sup>[22]</sup> there is some evidence that the more potent systems involve ruthenium(III) and ruthenium(V) complexes.<sup>[20d, 23]</sup> As the main difference between corroles and porphyrins is that the former stabilize complexes with one oxidation state than porphyrins,<sup>[11]</sup> we expected to obtain ruthenium(III) corroles that would display unique chemistry. Indeed, we have already demonstrated that iron(III) corroles are more efficient cyclopropanation catalysts than iron(III) porphyrins and that the iron(IV) complex of H<sub>3</sub>(tpfc) is the best catalyst that has been found for aziridination of olefins by Chloramine-T.<sup>[15a,b, 8b]</sup>

First, we tried to insert ruthenium into H<sub>3</sub>(tpfc) with either [Ru<sub>3</sub>(CO)<sub>15</sub>] or [Ru<sub>2</sub>Cl<sub>4</sub>(CO)<sub>6</sub>] as metal source. We examined a variety of solvents with different polarities and boiling points (benzene, toluene, pyridine, DMF), but a well-defined product was not obtained. However, when we employed [Ru(cod)Cl<sub>2</sub>]<sub>x</sub>, which was introduced by Guilard and co-workers for the same purpose with a different corrole,<sup>[18]</sup> the binuclear complex [Ru(tpfc)<sub>2</sub>] was isolated in reasonable yield (50%). Furthermore, TLC analyses during the reaction indicated that [Ru(tpfc)<sub>2</sub>] and an additional complex are present in an about 1:1 ratio. Since this product was likely to be the desired mononuclear corrole, we applied the same approach that produced iron(III) and cobalt(III) complexes of H<sub>3</sub>(tpfc),<sup>[8b, 9]</sup> that is, addition of pyridine prior to solvent



Scheme 1. Synthesis of mononuclear and binuclear ruthenium corroles.

evaporation, as eluent additive in the chromatographic step, and in the recrystallization mixture. However, even material that had excess of pyridine at all times converted gradually into a mixture of [Ru(tpfc)<sub>2</sub>] and other unidentified products.

An alternative approach that we considered as suitable for isolating this apparently very reactive complex was to use NO. This approach was based on three assumptions: NO will block at least one metal coordination site, it will reduce the reactivity of the metal due to its strong *trans*-effect and *trans*-influence, and the resulting nitrosyl complex would be diamagnetic and, therefore, easy to characterize. This hypothesis proved correct. When TLC analyses indicated that the free-base corrole was fully consumed, NO gas was introduced into the hot solution. Any [Ru(tpfc)<sub>2</sub>] that was already formed was not affected by this treatment (also independently confirmed on isolated material), but the other major component (green) in the TLC analysis became red. The crude reaction mixtures were subjected to column chromatography and both [Ru(tpfc)<sub>2</sub>] and [Ru(tpfc)(NO)] were isolated. In the case of H<sub>3</sub>(tdcc), only [Ru(tdcc)(NO)] was isolated (Scheme 1). All three complexes have a certain affinity for additional ligands, as revealed from both spectroscopy and crystallography.

## Abstract in Hebrew:

המטרה הראשית של מחקר זה הייתה הכנה של קומפלקסי רותניום קורול חד-מתכתיים, בגלל הפוטנציאל המוכח של קומפלקסים [Ru(COD)Cl<sub>2</sub>]<sub>x</sub> שימוש ב- שימוש ב- אנלוגיים של פורפירינים בקטליזה. שימוש ב- כמקור המתכת, אפשר את ההכנה של הקומפלקסי ניטרזיל החד-מתכתיים Ru(tpfc)(NO) ו-Ru(tdcc)(NO) וגם של הקומפלקס הדו-מתכתי [Ru(tpfc)<sub>2</sub>]. ספקטרא התמיג של שלשת הקומפלקסים ממחישים בבירור את הדיא-מגנטיות שלהם, בהתאמה לקיומו של קשר משולש בין יוני המתכת ב-[Ru(tpfc)<sub>2</sub>] ולציפיות עבור קומפלקסי {MNO}<sup>6</sup>. חיזוק נוסף לתכונות אלו, התקבל מתוך ספקטרה האינפרא אדום של יחידות ה-Ru-NO, מדידות אלקטרוכימיות של כל הקומפלקסים והמבנים המולקולריים של [Ru(tpfc)<sub>2</sub>] ו-Ru(tpfc)(NO). בהשוואת המאפיינים הספקטרוסקופיים והמבניים של הקומפלקסים החדשים עם ברזל קורולים אנלוגיים וגם עם ברזל ורותניום פורפירינים, מצביעים על כך שיהיה קשה לבודד קומפלקסי רותניום קורול ללא ליגנדות המסוגלות לקבל אלקטרוני π.

**NMR spectroscopy:** Room temperature <sup>1</sup>H and <sup>19</sup>F NMR spectra of [Ru(tpfc)<sub>2</sub>], a ruthenium(III)–ruthenium(III) dimer, are shown in Figures 1a and 2a, respectively. The chemical shifts are similar to those found in diamagnetic metal complexes of H<sub>3</sub>(tpfc),<sup>[8b]</sup> but the <sup>1</sup>H and some of the <sup>19</sup>F resonances are broad. There are two possible reasons for this phenomenon: an equilibrium (or quantum mechanical mixing) between dia- and paramagnetic states or some dynamic processes. These may be distinguished by the response of the spectra to measurements at other temperatures. An example of the former condition was found in Cu(corrole) complexes: sharp and nonparamagnetically shifted signals at low temperatures broaden and shift (by several ppm) as the temperature is raised.<sup>[11]</sup> This phenomenon was analyzed as reflecting a ground state that consists of a square-planar copper(III) ion (d<sup>8</sup>, diamagnetic) that is complexed by a closed-shell corrole trianion, and a low-lying excited state of a Cu<sup>II</sup> corrole radical.

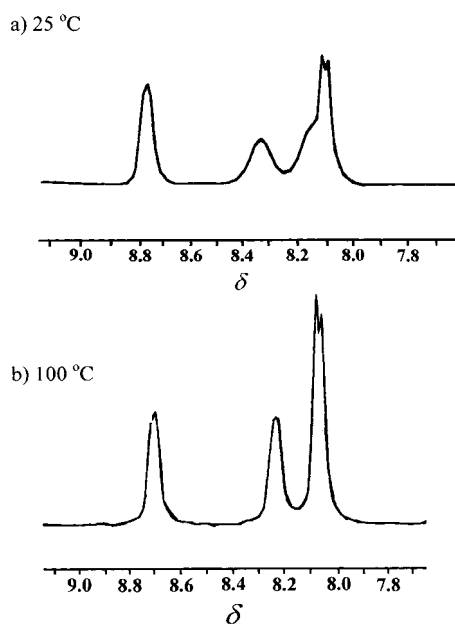


Figure 1.  $^1\text{H}$  NMR spectra of  $[\{\text{Ru}(\text{tpfc})_2\}]$  in  $[\text{D}_8]\text{toluene}$  at a) 25 °C and b) 100 °C.

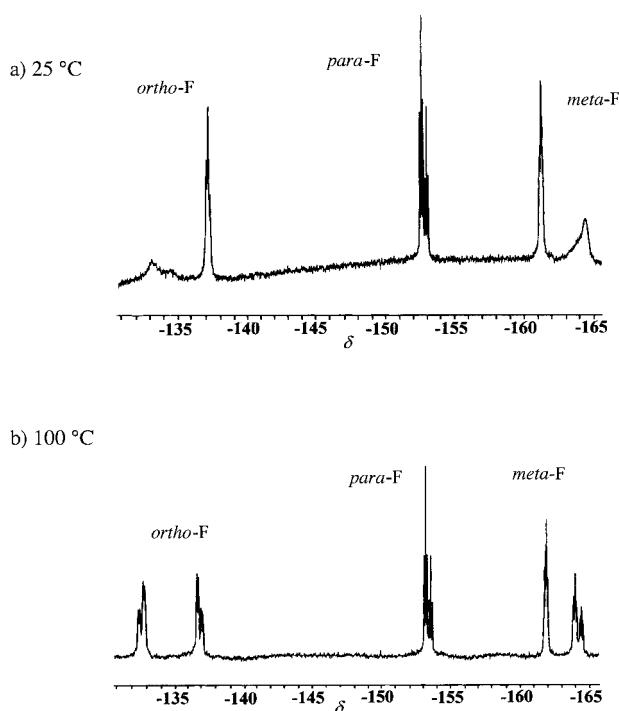
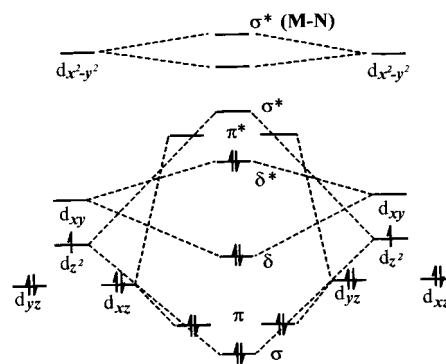


Figure 2.  $^{19}\text{F}$  NMR spectra of  $[\{\text{Ru}(\text{tpfc})_2\}]$  in  $[\text{D}_8]\text{toluene}$  at a) 25 °C and b) 100 °C.

If the broad signals were due to some slow rotational or conformational processes, the signals should actually appear sharper at higher temperatures. In fact, the sharper resonances observed in the spectra recorded at 100 °C (Figures 1b and 2b) clearly support the second possibility, that is, that the signal broadness at lower temperatures is due to a dynamic process that is slow on the NMR timescale. A reasonable hypothesis is to attribute it to the mutual rearrangement of the inner F atoms from each half of the complex; due to their closeness in space they should have a significant affect on each other.

Another important piece of information that can be deduced from the  $^{19}\text{F}$  NMR spectrum of  $[\{\text{Ru}(\text{tpfc})_2\}]$  is that structure of the complex must contain a  $C_2$  symmetry axis. This is reflected by the fact that the six  $\text{C}_6\text{F}_5$  substituents are divided into two magnetically equivalent groups, which consist of four and two rings each. There are then only two possible geometries,  $C_{2v}$  and  $D_{2h}$ , in which the two individual  $\text{N}_4$  coordination cores overlap in a staggered and eclipsed fashion, respectively. The diamagnetism of  $[\{\text{Ru}(\text{tpfc})_2\}]$  is consistent with both geometries, in which the strong  $d^5-d^5$  coupling leads to one  $\sigma$ , two  $\pi$ , one  $\delta$ , and one  $\delta^*$  bonds, with a bond order of three (Scheme 2).<sup>[24]</sup> This is also consistent with its X-ray structure and electrochemistry, which are discussed in the later sections.



Scheme 2. Correlation diagram for a  $\text{Ru}^{\text{III}}-\text{Ru}^{\text{III}}$  dimer under  $D_{4h}$  symmetry (an analogous diagram holds for lower symmetries as well).

The  $^1\text{H}$  NMR spectra of  $[\text{Ru}(\text{tpfc})(\text{NO})]$  and  $[\text{Ru}(\text{tdcc})(\text{NO})]$ , which are shown in Figure 3, demonstrate that the nitrosyl complexes are diamagnetic. This is consistent with the

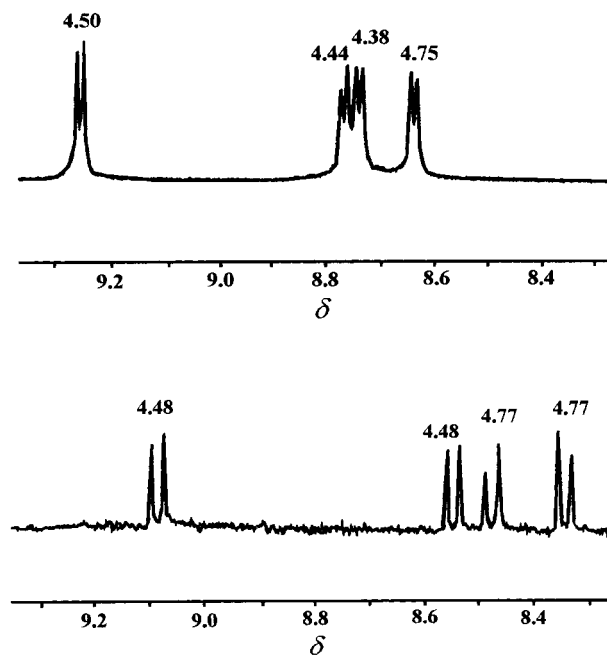


Figure 3. Top:  $^1\text{H}$  NMR spectra of  $[\text{Ru}(\text{tpfc})(\text{NO})]$  (in  $\text{CDCl}_3$ , 400 MHz, 25 °C). Bottom: Partial  $^1\text{H}$  NMR spectra (resonances of  $\beta$ -pyrrole protons only) of  $[\text{Ru}(\text{tdcc})(\text{NO})]$  (in  $\text{CDCl}_3$ , 200 MHz, 25 °C). Numbers indicate  $J$  coupling constant.

prediction for  $\{MNO\}^6$  complexes and a linear arrangement of the Ru-N-O moiety. However, the IR spectra of both complexes and the  $^{19}\text{F}$  NMR spectrum of  $[\text{Ru}(\text{tpfc})(\text{NO})]$  indicate the presence of more than one species. This suggests that the isolated complexes contain a variety of ligands *trans* to NO, reminiscent of similar findings in neutral (carbonyl)-ruthenium(II) porphyrins and in positively charged (nitrosyl)ruthenium porphyrins.<sup>[25]</sup> This is supported by the observation that the addition of pyridine or THF to the  $[\text{RuNO}]$  complexes in solution leads to significant changes in their color and electronic spectra. Accordingly, the  $^{19}\text{F}$  NMR of  $[\text{Ru}(\text{tpfc})(\text{NO})]$  was measured in  $[\text{D}_5]\text{pyridine}$ . The spectrum, shown in Figure 4, shows that only one species is present in solution, and the different sets of *ortho*-F atoms are consistent with the different environment above and below the corrole plane due to a *trans* arrangement of NO and pyridine in  $[\text{Ru}(\text{tpfc})(\text{NO})([\text{D}_5]\text{py})]$ . The NO stretching frequencies in pyridine are 1835 and 1827  $\text{cm}^{-1}$ , for  $[\text{Ru}(\text{tpfc})(\text{NO})(\text{py})]$  and  $[\text{Ru}(\text{tdcc})(\text{NO})(\text{py})]$ , respectively. These values are significantly lower than that of the isoelectronic porphyrin complex  $[\text{Ru}(\text{tpp})(\text{NO})(\text{py})]^+$  (1879  $\text{cm}^{-1}$ ; tpp = dianion of 5,10,15,20-tetraphenylporphyrin), which has more electron-rich *meso*-

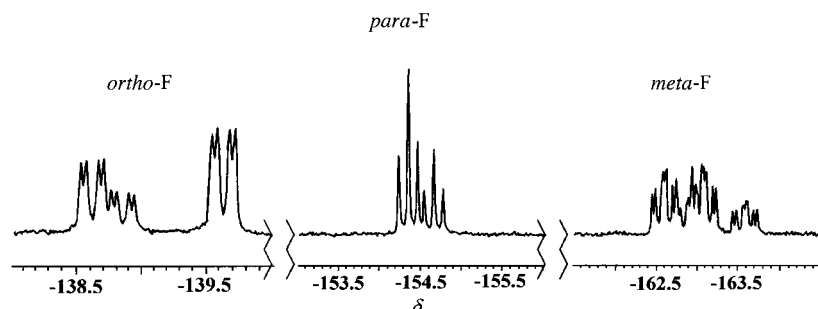


Figure 4.  $^{19}\text{F}$  NMR spectra of  $[\text{Ru}(\text{tpfc})(\text{NO})]$  (in  $[\text{D}_5]\text{pyridine}$ , 200 MHz, 25 °C).

aryl substituents.<sup>[26]</sup> Still, the values of 1790 and 1783  $\text{cm}^{-1}$  for  $[\text{Fe}(\text{tpfc})(\text{NO})]$  and  $[\text{Fe}(\text{tdcc})(\text{NO})]$ , respectively, are more than 100  $\text{cm}^{-1}$  lower than for analogous porphyrin complexes.<sup>[25, 8c]</sup> This suggests that while in both cases back-donation to NO is stronger in metal ions that are chelated by corroles than by porphyrins, the effect is smaller for ruthenium than for iron. In any case, the linearity of the Ru-N-O moiety, which is predicted by IR spectroscopy and electron-counting, was confirmed by the X-ray structure analysis of  $[\text{Ru}(\text{tpfc})(\text{NO})]$ .

**Electrochemistry:** The cyclic voltammograms (CVs) of  $[\text{Ru}(\text{tpfc})(\text{NO})]$  and  $[\text{Ru}(\text{tdcc})(\text{NO})]$  are shown in Figures 5 and 6, respectively. One oxidation and two reduction waves are evident in the CVs of both complexes. The half-wave potentials of  $[\text{Ru}(\text{tpfc})(\text{NO})]$  are more positive (easier to reduce and harder to oxidize) than for  $[\text{Ru}(\text{tdcc})(\text{NO})]$ , as expected for a corrole with more electron-withdrawing *meso*-substituents. Based on a comparison with non-transition-metal complexes of tpfc, in which the corrole-centered redox processes occur above 1.0 V and below -1.0 V,<sup>[8b]</sup> the first reduction ( $[\text{Ru}(\text{tpfc})(\text{NO})]$ :  $E_{1/2} = -0.42$  V,  $[\text{Ru}(\text{tdcc})(\text{NO})]$ :  $E_{1/2} = -0.50$  V) and the first oxidation waves ( $[\text{Ru}(\text{tpfc})$

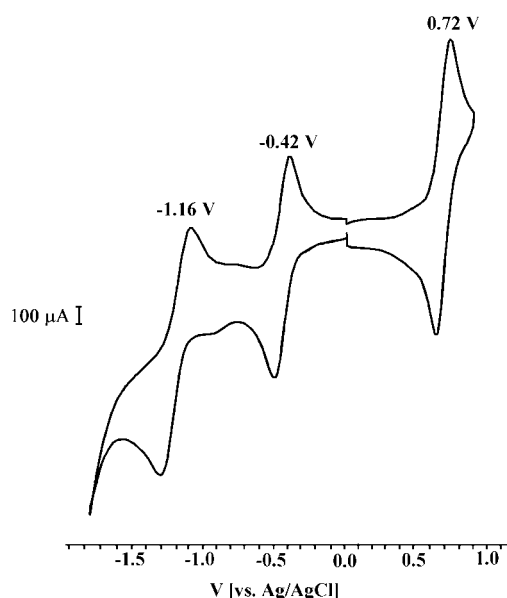


Figure 5. Cyclic voltammogram of  $[\text{Ru}(\text{tpfc})(\text{NO})]$  in 0.05M TBAP/ $\text{CH}_3\text{CN}$  and half-wave potentials of the redox couples. Scan rate: 100  $\text{mV s}^{-1}$ .

$(\text{NO})$ :  $E_{1/2} = 0.72$  V,  $[\text{Ru}(\text{tdcc})(\text{NO})]$ :  $E_{1/2} = 0.57$  V) may be assigned as reflecting metal-centered processes. This differs from the situation in iron nitrosyl corroles, in which the first reduction is metal-centered (at  $E_{1/2}$  of 0.0 and -0.41 V for  $[\text{Fe}(\text{tpfc})(\text{NO})]$  and  $[\text{Fe}(\text{oec})(\text{NO})]$  (oec = trianion of 2,3,7,8,12,13,17,18-octaethylcorrole), respectively), but in

which oxidation takes place on the corrole (at  $E_{1/2}$  of 1.07 and 0.61 V for  $[\text{Fe}(\text{tpfc})(\text{NO})]$  and  $[\text{Fe}(\text{oec})(\text{NO})]$ , respectively).<sup>[27]</sup> An additional comparison is with the isoelectronic porphyrin complexes  $[\text{Ru}(\text{tpp})(\text{NO})(\text{L})]^+$ , in which  $\text{L} = \text{py}$  or  $\text{H}_2\text{O}$ . While these complexes are more easily reduced

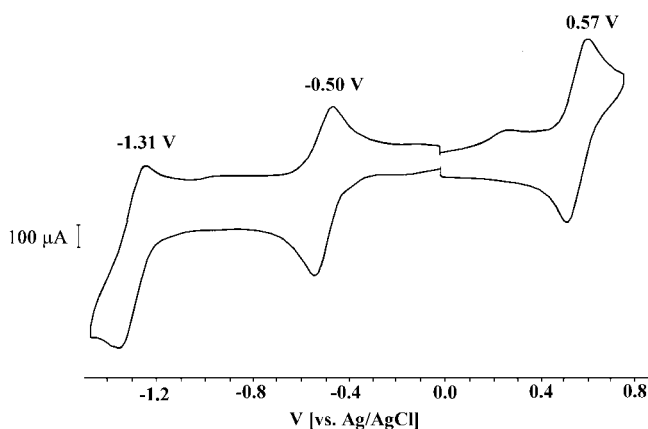


Figure 6. Cyclic voltammogram of  $[\text{Ru}(\text{tdcc})(\text{NO})]$  in 0.05M TBAP/ $\text{CH}_3\text{CN}$  with half wave potentials of the redox couples. Scan rate: 200  $\text{mV s}^{-1}$ .

( $E_{1/2} = -0.29$  V, data for  $L = \text{py}$ ), their oxidation potentials are higher ( $E_{1/2} = 1.26$  V, data for  $L = \text{H}_2\text{O}$ ) than those of the corrole complexes.<sup>[26]</sup> This demonstrates a unique feature of corroles as ligands, that is, the destabilization of low-valent and stabilization of high-valent metal oxidation states.

The electrochemistry of  $[\{\text{Ru}(\text{tpfc})\}_2]$  is richer, and the CV is shown in Figure 7. The half-wave potentials of the first three redox processes (starting with  $E_{1/2} = -1.21$  V) are similar to that of  $[\text{Ru}(\text{tpfc})(\text{NO})]$ , suggesting that the Ru–Ru and the Ru–NO bonds exert a similar electronic effect on the metal. A different comparison is with the well-known porphyrin analogues,  $[\{\text{Ru}(\text{tpp})\}_2]$  and  $[\{\text{Ru}(\text{oep})\}_2]$  (oep = dianion of octaethylporphyrin), which have double bonds between the  $\text{Ru}^{\text{II}}$  ions.<sup>[28–30]</sup>

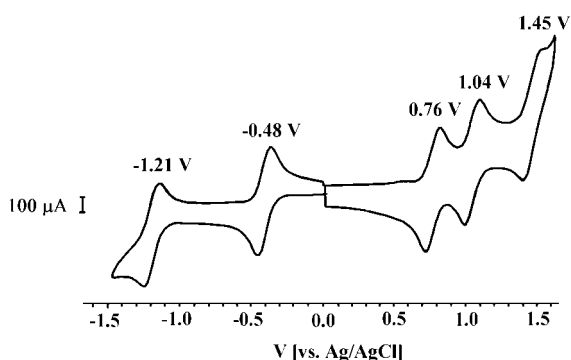


Figure 7. Cyclic voltammogram of  $[\{\text{Ru}(\text{tpfc})\}_2]$  in 0.05 M TBAP/ $\text{CH}_3\text{CN}$  with half wave potentials of the redox couples. Scan rate:  $100 \text{ mV s}^{-1}$ .

Unfortunately, only the electrochemistry of  $[\{\text{Ru}(\text{oep})\}_2]$  has been reported.<sup>[30]</sup> Nevertheless, five electrochemically reversible one-electron redox couples are evident in both  $[\{\text{Ru}(\text{tpfc})\}_2]$  and  $[\{\text{Ru}(\text{oep})\}_2]$  (in  $\text{CH}_2\text{Cl}_2$ ).<sup>[30]</sup> Similar to the assignment given for  $[\{\text{Ru}(\text{oep})\}_2]$ , we propose that the first reduction and oxidation couples are metal-centered, because of the relatively low half-wave potentials at  $-0.48$  V and  $+0.76$  V, respectively. As for the oxidation couple at  $1.04$  V, we are unable as yet to assign it to the oxidation of the corrole or of the metal. The latter assignment would correspond to a  $\text{Ru}^{\text{IV}}-\text{Ru}^{\text{IV}}$  dimer with a bond order of four, but we await the isolation of the chemically oxidized complex (as was performed for porphyrins) for a definitive answer.<sup>[30]</sup>

**Structural aspects:** The molecular structure of  $[\{\text{Ru}(\text{tpfc})\}_2]$  is presented in Figure 8. The molecules are located on crystallographic inversion centers, and the two Ru–corrole fragments are structurally identical. The triple Ru–Ru bond, which forms the center of inversion of the complex, is  $2.182 \text{ \AA}$ ; this is comparable to the bond length in Guillard's binuclear ruthenium corrole ( $2.166 \text{ \AA}$ )<sup>[18]</sup> and is significantly shorter than that of the Ru–Ru double bond ( $2.408 \text{ \AA}$ ) in the well-known  $[\text{Ru}(\text{oep})_2]$  porphyrin complex, or of that in  $[\{\text{Ru}(\text{tpp})\}_2]^+$ , which has a Ru–Ru bond order of 2.5 and length of  $2.293 \text{ \AA}$ .<sup>[24, 31]</sup> In order to minimize the steric repulsions between the macrocycles, the two corrole units are oriented in a staggered manner with respect to each other, so that the  $\text{C}_6\text{F}_5$  substituent at C10 of one corrole is placed

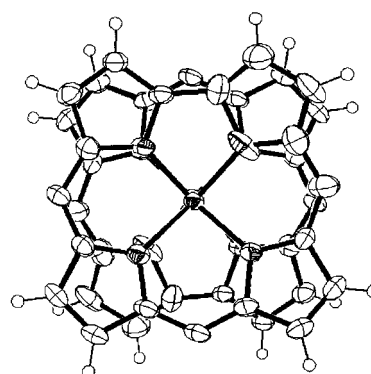
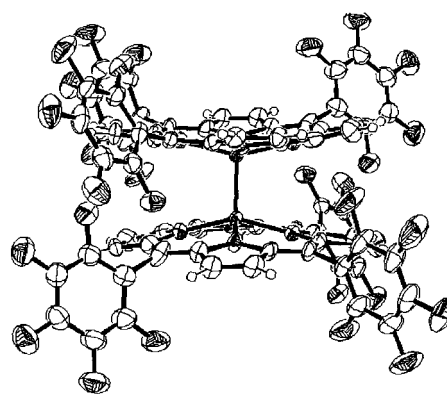


Figure 8. Full side-view and partial top-view of the molecular structure of  $[\{\text{Ru}(\text{tpfc})\}_2]$  as it exists in the crystal. The ellipsoids represent atomic displacement parameters at the 50% probability level.

above the free space near the C1–C19 bond of the other corrole. The aryl substituents at C5 and C15 of the two corroles are placed one above the other, and to avoid edge–edge collision, they are rotated by  $17$  and  $25^\circ$  from perpendicularity with respect to the corrole macrocycle. The corresponding dihedral angles between the planes of the aryl rings and the corrole moiety are  $73.0$ ,  $78.6$ , and  $65.3^\circ$ , for the substituents at C5, C10, and C15, respectively. The aryl arms interlock the corrole dimer in this ordered conformation (which is probably the source of the dynamic process in solution, as discussed previously), unlike the rotationally disordered Guillard's complex, which lacks such aryl "stoppers".<sup>[18]</sup> The Ru ion is significantly displaced from the corrole framework along the axial direction towards the other ruthenium ion. It deviates by  $0.50 \text{ \AA}$  from the plane of the four pyrrole nitrogen atoms, if one assumes a square-pyramidal coordination environment and imparts a domed conformation to each half of the dimeric species. This also involves a slight upward rotation of the pyrrole rings with respect to the mean plane of the corrole macrocycle towards the metal, the inner N atoms lying on average  $0.3 \text{ \AA}$  above the mean plane of the carbon-only C<sub>19</sub> framework. The benzene molecules are located near and parallel to the concave surface of the two corrole rings of the dimers, as also found in ruthenium porphyrins.<sup>[32]</sup> The distances of the benzene carbon atoms that approach the concave surface of the corrole in the dimer vary from  $3.18$ – $3.54 \text{ \AA}$  from the mean plane of the four

pyrrole nitrogen atoms and from 2.86–3.24 Å from the mean plane of the C<sub>19</sub> corrole framework. In comparison to other porphyrin–metal complexes (Cr, Zn, Mn) these separations are much shorter, and indicate a strong  $\pi$ – $\pi$  interaction.<sup>[33]</sup>

The molecular structure of [Ru(tpfc)(NO)], which is shown in Figure 9, has similar features. The Ru ion is five-coordinate, and is displaced from the corrole ring towards the axial NO ligand. In the two independent species occurring in the crystal

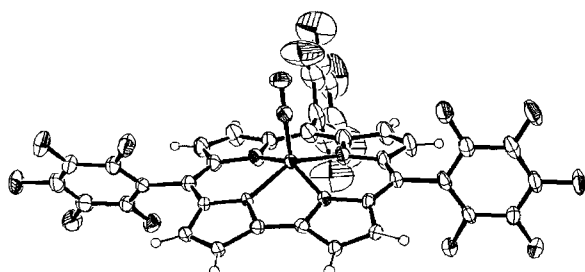


Figure 9. Crystal structure of the mononuclear ruthenium-nitrosyl corrole, [Ru(tpfc)(NO)]. The ellipsoids represent atomic displacement parameters at the 50% probability level.

it lies 0.54 Å above the plane of the four pyrrole nitrogen atoms, which in turn are placed an average of 0.2 Å above the mean plane of the C<sub>19</sub> corrole ring. In this domed structure, the Ru–NO bonds are essentially linear with bond angles of 178.2 and 179.3°. The aryl substituents are aligned in a roughly perpendicular manner with respect to the corrole macrocycle (with a single exception). Five of the corresponding dihedral angles between the aryl and the C<sub>19</sub> corrole planes are within 77.3–85.0°, values that are typical of closed-shell corrole complexes, while the sixth aryl ring is more twisted (64.7°) due to crystal packing constraints. In both our structures the bond lengths between Ru and the N-pyrrole atoms that are adjacent to the C1–C19 bond are slightly shorter than to the other pyrrole nitrogen atoms, as is commonly observed in structures of corrole complexes with metal ions.

It is interesting to compare the main features of [Ru(tpfc)(NO)] with the recently reported molecular structures of the iron–nitrosyl complexes of tpfc and tdcc (see Table 1).<sup>[8c]</sup> The metal out-of-plane displacement of ruthenium is almost 0.1 Å larger than of iron, which is accompanied by larger metal–N(corrole) bond lengths in the [Ru(tpfc)(NO)] complex. In addition, both the average bond lengths in the M–N–O moiety of [Ru(tpfc)(NO)] (M–NO: 1.715 Å, N–O: 1.175 Å) are longer than in [Fe(tpfc)(NO)] (M–NO: 1.643 Å, N–O:

1.165 Å), and are consistent with the fact that ruthenium(II) is a weaker  $\sigma$  acceptor and a stronger  $\pi$  donor than iron(II). The affinity of the nitrosyl complexes to amines other than pyridine (such as imidazole) is an issue that will be addressed in future studies.

## Conclusion

We report a method for the preparation of mononuclear ruthenium corroles that is based on the treatment of reaction mixtures of triarylcorroles and [Ru(cod)Cl<sub>2</sub>]<sub>x</sub> with NO(g). Novel nitrosyl complexes, [Ru(tpfc)(NO)] and [Ru(tdcc)(NO)], were isolated in about 40% yield and characterized by spectroscopy and electrochemistry. A binuclear [Ru(tpfc)<sub>2</sub>] complex was also obtained in 50% yield in the absence of treatment with NO(g). Additional information was obtained from the molecular structures of [Ru(tpfc)<sub>2</sub>] and [Ru(tpfc)(NO)]. The data is consistent with a triple bond between the metal ions in [Ru(tpfc)<sub>2</sub>] and a linear arrangement of the M–NO moiety in [Ru(tpfc)(NO)] and [Ru(tdcc)(NO)], as expected for [MNO]<sub>6</sub> complexes. A comparison of the NO stretching frequencies in the ruthenium- and iron-nitrosyl corroles with analogous porphyrins shows that in both cases back-donation to NO is stronger in metal corroles, and that the effect is smaller for ruthenium than for iron. The metal out-of-plane displacement in [Ru(tpfc)(NO)] corrole is higher than in the iron analog [Fe(tpfc)(NO)], and this suggests that mononuclear ruthenium corroles without  $\pi$ -accepting ligands will be hard to obtain.

## Experimental Section

**Physical methods:** The <sup>1</sup>H NMR and <sup>19</sup>F NMR spectra were recorded on a Bruker AM 200 and Bruker AM 400, operating at 200 and 400 MHz for <sup>1</sup>H and 188 MHz for <sup>19</sup>F NMR. Chemical shifts are reported in ppm relative to residual hydrogen atoms in the deuterated solvents: 7.24, 7.15, and 7.00 ppm for chloroform, benzene, and toluene, respectively, for <sup>1</sup>H NMR spectra and relative to CFC<sub>3</sub> ( $\delta$  = 0.00 ppm) in <sup>19</sup>F NMR spectra. Electronic spectra were recorded on a HP 8452A diode array spectrophotometer. Mass Spectrometry was performed on a Finnigan mat TSQ 70 instrument with isobutane as carrier gas and IR measurements on a FT-IR Bruker Vector 22.

Redox potentials were determined on substrate ( $\approx$ 0.5 mm) in a solution of *n*-tetrabutylammonium perchlorate (0.05 M) in acetonitrile by cyclic voltammetry (CV) at ambient temperatures on a home-made voltammograph under an Ar atmosphere. A three-electrode system was used with a platinum working electrode, a platinum wire counter electrode, and Ag/

Table 1. Selected parameters for all structurally characterized metal nitrosyl complexes of triarylcorroles.

Complex	[Ru(tpfc)(NO)] <sup>[a]</sup>	[Fe(tpfc)(NO)] <sup>[a]</sup>	[Fe(tdcc)(NO)]
M–N(corrole) bond length range [Å]	1.961–1.999	1.893–1.926	1.898–1.922
<i>meso</i> -aryl-corrole angles [°]	64.7, 77.3–85.0	64.7, 84.5, 81.3, 78.1, 86.2, 77.3	87.8, 82.3, 83.0
M–NO angle [°]	178, 179	177, 178	172
M–NO bond length [Å]	1.712, 1.718	1.639, 1.648(4)	1.641(4)
M out-of-plane displacement [Å] <sup>[b]</sup>	0.54	0.465, 0.464(1)	0.452(2)
NO bond length [Å]	1.173, 1.177	1.164, 1.166	1.169
$\tilde{\nu}$ [cm <sup>-1</sup> ]	1827 <sup>[c]</sup>	1790 <sup>[d]</sup>	1783 <sup>[d]</sup>

[a] There are two crystallographically independent corrole species in the asymmetric unit of these structures. [b] Plane defined by the four inner N atoms. [c] Measured in pyridine, wherein the complex exists as [Ru(tpfc)(NO)(py)]. In non-coordinating solvents and in KBr pellets, more than one NO stretching frequency was obtained due to the presence of several *trans*-ligands. [d] KBr pellet.

AgCl as the reference electrode. The redox potentials are reported versus the ferrocene/ferrocenium redox couple observed at 0.4 V versus Ag/AgCl. Other experimental conditions are reported in the legends of the corresponding spectra.

**Materials:** TBAP (tetrabutyl ammonium perchlorate: Fluka; recrystallized three times from absolute ethanol), 2-methoxyethanol (Fluka), CH<sub>3</sub>CN (BioLab), triethylamine (Spectrum), [[Ru(cod)Cl<sub>2</sub>]<sub>2</sub>] (Aldrich) and deuterated solvents (Aldrich and Cambridge Isotopes products) were used as received.

**Synthetic methods:** The synthetic details for the preparation of H<sub>3</sub>(tpfc) and H<sub>3</sub>(tdcc) are provided in our previous publications.<sup>[1a,b]</sup> NO gas was obtained from the reaction between NaNO<sub>2</sub> and H<sub>2</sub>SO<sub>4</sub>, purified from NO<sub>2</sub> impurities by using a 30% solution of NaOH, and dried by passing through solid NaOH.

**Synthesis of [[Ru(tpfc)]<sub>2</sub>] and [Ru(tpfc)(NO)] (standard procedure):** Under argon gas, a solution of H<sub>3</sub>(tpfc) (100 mg, 0.126 mmol) in 2-methoxyethanol (20 mL) was heated under reflux. Excess [[Ru(cod)Cl<sub>2</sub>]<sub>2</sub>] (176 mg, 0.63 mmol) and triethylamine (0.054 mL, 0.38 mmol) were added to the hot solution in one portion. TLC (silica: *n*-hexane/dichloromethane, 3:2) analyses showed that the starting material was fully consumed within about 30 min. A stream of dried NO was bubbled through the hot solution for about 5 min and then replaced by argon. The solvent was evaporated. Purification and separation of the products was performed by column chromatography on silica gel with a solvent mixture of *n*-hexane and dichloromethane. Solvent ratios of 7:1 and 4:1, respectively, were used to isolate the red-brown [[Ru(tpfc)]<sub>2</sub>] (first fraction) and wine-red [Ru(tpfc)(NO)] (second fraction). Solvent evaporation and recrystallization from CH<sub>2</sub>Cl<sub>2</sub>/*n*-heptane mixtures resulted in 44 mg (24.6 μmol, 39% yield) of [[Ru(tpfc)]<sub>2</sub>] and 35 mg (37.8 μmol, 30% yield) of [Ru(tpfc)(NO)]. Dark red diffraction-quality crystals of [[Ru(tpfc)]<sub>2</sub>] were obtained from a mixture of benzene and *n*-heptane. When the same procedure was applied, without the introduction of NO, the yield of isolated [[Ru(tpfc)]<sub>2</sub>] was 50%.

**[[Ru(tpfc)]<sub>2</sub>]:** <sup>1</sup>H NMR (200 MHz, CDCl<sub>3</sub>, RT): δ = 8.88 (d, <sup>3</sup>J(H,H) = 4.28 Hz, 4H), 8.28 (brs, 4H), 8.21 (d, <sup>3</sup>J(H,H) = 4.55 Hz, 4H), 8.16 ppm (brs, 4H); <sup>19</sup>F NMR (188 MHz, CDCl<sub>3</sub>, RT) δ = -133.10 (brs, 6F; *ortho*-F), -137.31 (d, <sup>3</sup>J(F,F) = 16.73 Hz, 6F; *ortho*-F), -152.70 (m, 6F; *para*-F), -161.68 (m, 6F; *meta*-F), -163.102 and -163.70 ppm (brs, 3F + 3F; *meta*-F); <sup>19</sup>F NMR (188 MHz, [D<sub>3</sub>]toluene, 100 °C) δ = -132.57 (d, <sup>3</sup>J(F,F) = 23.69 Hz, 2F; *ortho*-F), -132.90 (d, <sup>3</sup>J(F,F) = 23.69 Hz, 4F; *ortho*-F), -136.74 (d, <sup>3</sup>J(F,F) = 21.06 Hz, 4F; *ortho*-F), -137.05 (d, <sup>3</sup>J(F,F) = 19.93 Hz, 2F; *ortho*-F), -153.16 (t, <sup>3</sup>J(F,F) = 20.49 Hz, 4F; *para*-F), -153.54 (t, <sup>3</sup>J(F,F) = 20.30 Hz, 2F; *para*-F), -161.89 (m, 6F; *meta*-F), -163.97 (td, <sup>3</sup>J(F,F) = 22.94 Hz, <sup>4</sup>J(F,F) = 8.08 Hz, 4F; *meta*-F), -164.45 ppm (td, <sup>3</sup>J(F,F) = 23.12 Hz, <sup>4</sup>J(F,F) = 8.08 Hz, 2F; *meta*-F); UV/Vis (CH<sub>2</sub>Cl<sub>2</sub>): λ<sub>max</sub> (ε × 10<sup>-4</sup>) = 332 (9.86), 398 (7.91), 538 nm (1.60); MS (DCI<sup>+</sup>): *m/z* (%): 1791 (100) [M<sup>+</sup>+H]; MS (DCI<sup>-</sup>): *m/z* (%): 1790 (100) [M<sup>-</sup>].

**[Ru(tpfc)(NO)]:** <sup>1</sup>H NMR (400 MHz, CDCl<sub>3</sub>, RT): δ = 9.26 (d, <sup>3</sup>J(H,H) = 4.50 Hz, 2H), 8.77 (d, <sup>3</sup>J(H,H) = 4.44 Hz, 2H), 8.74 (d, <sup>3</sup>J(H,H) = 4.38 Hz, 2H), 8.64 ppm (d, <sup>3</sup>J(H,H) = 4.75 Hz, 2H); <sup>19</sup>F NMR (188 MHz, CDCl<sub>3</sub>, RT): δ = -136.98 (dd, <sup>3</sup>J(F,F) = 23.12 Hz, <sup>4</sup>J(F,F) = 4.89 Hz, 2F; *ortho*-F), -137.25 (dd, <sup>3</sup>J(F,F) = 23.69 Hz, <sup>4</sup>J(F,F) = 6.02 Hz, 1F; *ortho*-F), -138.02 (m, 3F; *ortho*-F), -152.36 (m, 3F; *para*-F), -161.40 ppm (m, 6F; *meta*-F); UV/Vis (CH<sub>2</sub>Cl<sub>2</sub>): λ<sub>max</sub> (ε × 10<sup>-4</sup>) = 406 (6.81), 538 nm (1.74); MS (DCI<sup>+</sup>): *m/z* (%): 926 (100) [M<sup>+</sup>+H]; MS (DCI<sup>-</sup>): *m/z* (%): 925 (100) [M<sup>-</sup>]; IR (pyridine): ν<sub>NO</sub> = 1835 cm<sup>-1</sup>.

**Synthesis of [Ru(tdcc)(NO)]:** This material was prepared by the same method as described above for [Ru(tpfc)(NO)] (with 100 mg of pure H<sub>3</sub>(tdcc)), but a binuclear complex was not obtained. The product was recrystallized from CH<sub>2</sub>Cl<sub>2</sub>/*n*-hexane mixtures and 35–40% yield (41–46 mg) of red crystals were obtained from repeated syntheses. <sup>1</sup>H NMR (200 MHz, CDCl<sub>3</sub>, RT): δ = 9.09 (d, <sup>3</sup>J(H,H) = 4.48 Hz, 2H; β-pyrrole H), 8.55 (d, <sup>3</sup>J(H,H) = 4.48 Hz, 2H; β-pyrrole H), 8.48 (d, <sup>3</sup>J(H,H) = 4.77 Hz, 2H; β-pyrrole H), 8.34 (d, <sup>3</sup>J(H,H) = 4.77 Hz, 2H; β-pyrrole H), 7.80 (td, <sup>3</sup>J(H,H) = 7.22 Hz, <sup>4</sup>J(H,H) = 2.13 Hz, 3H; *para*-H of *meso*-phenyl), 7.68 ppm (m, 6H; *meta*-H of *meso*-phenyl); UV/Vis (CH<sub>2</sub>Cl<sub>2</sub>): λ<sub>max</sub> (ε × 10<sup>-4</sup>) = 408 (2.79), 542 nm (0.7); MS (DCI<sup>+</sup>): *m/z* (%): 861 (100) [M<sup>+</sup>]; IR (pyridine): ν<sub>NO</sub> = 1827 cm<sup>-1</sup>; elemental analysis calcd (%) for [Ru(tdcc)(NO)]·py·2(C<sub>6</sub>H<sub>14</sub>)<sub>2</sub>, C<sub>54</sub>H<sub>50</sub>Cl<sub>6</sub>N<sub>6</sub>ORu: C 58.28, H 4.53, N 7.55; found C

57.82, H 4.75, N 7.36 (the hexane (≈20%) in the solid may be responsible for the relatively low ε values of the complex).

**Electrochemistry:** Cyclovoltammograms of [[Ru(tpfc)]<sub>2</sub>], [Ru(tpfc)(NO)], and [Ru(tdcc)(NO)] were obtained from approximately 0.5 mm substrate in 0.05 M TBAP/CH<sub>3</sub>CN solutions at scan rates of 100 or 200 V s<sup>-1</sup>. Those shown in Figure 5–7 were measured under an argon atmosphere, as in aerobic solutions only the first reduction and first oxidation waves were reversible.

**X-ray crystallography of [[Ru(tpfc)]<sub>2</sub>] and [Ru(tpfc)(NO)]:** Crystalline samples of [[Ru(tpfc)]<sub>2</sub>] and [Ru(tpfc)(NO)] were covered with a thin layer of light oil and cooled to 110 K in order to minimize both the escape of volatile crystallization solvents and thermal motion/structural disorder effects. The intensity data were measured on a Nonius KappaCCD diffractometer, and corrected for absorption. The structures were solved by either direct (SIR-97) or Patterson (DIRDIF-96) methods and refined by full-matrix least-squares method (SHELXL-97). Non-hydrogen atoms of the corroles were refined anisotropically. The hydrogen atoms were located in idealized positions, and were refined using a riding model with fixed thermal parameters ( $U_{ij} = 1.2 U_{ij}$  for the atom to which they are bonded). The two corrole compounds co-crystallized with additional guest/solvent components trapped, and severely disordered, in the lattice. Yet, in both cases the crystallographic analysis provided an unequivocal description of the respective Ru–corrole structures.

**[[Ru(tpfc)]<sub>2</sub>]:** 2[C<sub>37</sub>H<sub>8</sub>F<sub>15</sub>N<sub>4</sub>Ru·C<sub>6</sub>H<sub>6</sub>], *M*<sub>r</sub> = 1945.30, monoclinic, space group *P*2<sub>1</sub>/*n*, *a* = 15.9440(2), *b* = 16.437(3), *c* = 16.5280(3) Å, β = 110.894(2)°, *V* = 4046.7(1) Å<sup>3</sup>, *Z* = 2, *T* = 110(2) K, ρ<sub>calcd</sub> = 1.596 g cm<sup>-3</sup>, μ(MoKα) = 0.49 mm<sup>-1</sup>, 7380 unique reflections to 2θ<sub>max</sub> = 51.4°, 580 refined parameters, *R*<sub>1</sub> = 0.085 for 6269 observed reflections with *I* > 2σ(*I*); *R*<sub>1</sub> = 0.096 (*wR*<sub>2</sub> = 0.239) for all unique data. The benzene solvate exhibited partial rotational disorder (most probably of a dynamic nature), as was best exhibited by large-amplitude in-plane wagging motion of the C atoms (the main components of their thermal displacement parameters were 2–3 times larger than those of the corrole ring atoms). The final residual electron density map revealed several very diffuse peaks (< 1 e Å<sup>-3</sup>), which may represent minute amounts of severely disordered *n*-heptane solvent present in the crystal lattice, which could not be modeled. This may be the reason for the relatively high *R* factors.

**[Ru(tpfc)(NO)]:** C<sub>37</sub>H<sub>8</sub>F<sub>15</sub>N<sub>5</sub>ORu·C<sub>7</sub>H<sub>16</sub>, *M*<sub>r</sub> = 1024.75, triclinic, space group *P*1̄, *a* = 7.0670(1), *b* = 20.0520(4), *c* = 27.9430(6) Å, α = 91.87(1), β = 90.62(1), γ = 94.43(1)°, *V* = 3945.4(1) Å<sup>3</sup>, *Z* = 4, *T* = 110(2) K, ρ<sub>calcd</sub> = 1.725 g cm<sup>-3</sup>, μ(MoKα) = 0.51 mm<sup>-1</sup>, 17312 unique reflections to 2θ<sub>max</sub> = 55.0°, 1132 refined parameters, *R*<sub>1</sub> = 0.070 for 12316 observed reflections with *I* > 2σ(*I*); *R*<sub>1</sub> = 0.109 (*wR*<sub>2</sub> = 0.184) for all unique data.

The asymmetric unit consisted of two corrole species, one *n*-heptane on general position and two partial heptanes located on, and disordered about the centers of inversion. These solvent molecules were severely disordered, and their structure could not be precisely determined.

CCDC 182424 and 182425 contains the supplementary crystallographic data for the complexes [[Ru(tpfc)]<sub>2</sub>] and [Ru(tpfc)(NO)], respectively, in this paper. These data can be obtained free of charge via www.ccdc.cam.ac.uk/conts/retrieving.html (or from the CCDC, 12 Union Road, Cambridge CB2 1EZ, UK (fax: (+44)1223-336033; or deposit@ccdc.cam.ac.uk).

## Acknowledgement

This research was supported by the Israel Science Foundation under Grants 368/00 (ZG) and 68/01 (IG). Partial support by the Petroleum Research Fund (ACS) and “Technion VPR Fund—New York Metropolitan Research Fund” is also acknowledged (ZG).

- [1] a) Z. Gross, N. Galili, I. Saltsman, *Angew. Chem.* **1999**, *111*, 1530; *Angew. Chem. Int. Ed.* **1999**, *38*, 1427; b) Z. Gross, N. Galili, L. Simkhovich, I. Saltsman, M. Botoshansky, D. Bläser, R. Boese, I. Goldberg, *Org. Lett.* **1999**, *1*, 599; c) L. Simkhovich, I. Goldberg, Z. Gross, *J. Inorg. Biochem.* **2000**, *80*, 235; d) E. Steene, T. Wondimagn, A. Ghosh, *J. Inorg. Biochem.* **2002**, *88*, 113.

- [2] For the synthesis of corroles by the modified Rothmund method, see: a) R. Paolesse, L. Jaquinod, D. J. Nurco, S. Mini, F. Sagone, T. Boschi, K. M. Smith, *Chem. Commun.* **1999**, 1307; b) R. Paolesse, S. Nardis, F. Sagone, R. G. Khoury, *J. Org. Chem.* **2001**, *66*, 550.
- [3] For the synthesis of corrole by the condensation of the dypyrromethanes with aldehydes, see: a) J.-W. Ka, C.-H. Lee, *Tetrahedron Lett.* **2000**, *41*, 4609; b) J.-W. Ka, W.-S. Cho, C.-H. Lee, *Tetrahedron Lett.* **2000**, *41*, 8121; c) D. T. Gryko, *Chem. Commun.* **2000**, 2243; d) D. T. Gryko, K. Jadach, *J. Org. Chem.* **2001**, *66*, 4267; e) R. P. Brinas, C. Bruckner, *Synlett*, **2001**, *3*, 442; f) C. V. Asokan, S. Smeets, W. Dehaen, *Tetrahedron Lett.* **2001**, *42*, 4483.
- [4] For the synthesis of corroles and corrole-like molecules by other methods, see: a) B. Sridevi, S. J. Narayanan, T. K. Chandrashekar, U. English, K. Ruhlandt-Senge, *Chem. Eur. J.* **2000**, *6*, 2554; b) B. Ramdhanie, C. L. Stern, D. P. Goldberg, *J. Am. Chem. Soc.* **2001**, *123*, 9447; c) M. Broering, C. Hell, *Chem. Commun.* **2001**, 2336.
- [5] a) R. Paolesse, S. Licocchia, M. Fanciullo, E. Morgante, T. Boschi, *Inorg. Chem. Acta* **1993**, *203*, 107; b) N. M. Loim, E. V. Grishko, N. I. Pyshnograeva, E. V. Vorontsov, V. I. Sokolov, *Izv. Akad. Nauk. Ser. Khim.* **1994**, *5*, 925; c) E. Rose, A. Kossanyi, M. Quelquejeu, M. Soleilhavoup, F. Duwavran, N. Bernard, A. Lecas, *J. Am. Chem. Soc.* **1996**, *118*, 1567.
- [6] a) A. E. Meier-Callahan, H. B. Gray, Z. Gross, *Inorg. Chem.* **2000**, *39*, 3605; b) A. E. Meier-Callahan, A. J. DiBilio, L. Simkhovich, A. Mahammed, I. Goldberg, H. B. Gray, Z. Gross, *Inorg. Chem.* **2001**, *40*, 6788.
- [7] a) Z. Gross, G. Golubkov, L. Simkhovich, *Angew. Chem.* **2000**, *112*, 4211; *Angew. Chem. Int. Ed.* **2000**, *39*, 4045; b) J. Bendix, G. Golubkov, H. B. Gray, Z. Gross, *Chem. Commun.* **2000**, 1957; c) G. Golubkov, J. Bendix, H. B. Gray, A. Mahammed, I. Goldberg, A. J. DiBilio, Z. Gross, *Angew. Chem.* **2001**, *113*, 2190; *Angew. Chem. Int. Ed.* **2001**, *40*, 2132.
- [8] a) L. Simkhovich, N. Galili, I. Saltsman, I. Goldberg, Z. Gross, *Inorg. Chem.* **2000**, *39*, 2704; b) L. Simkhovich, A. Mahammed, I. Goldberg, Z. Gross, *Chem. Eur. J.* **2001**, *7*, 1041; c) L. Simkhovich, I. Goldberg, Z. Gross, *Inorg. Chem.* **2002**, *41*, 5433.
- [9] A. Mahammed, I. Giladi, I. Goldberg, Z. Gross, *Chem. Eur. J.* **2001**, *7*, 4259.
- [10] L. Simkhovich, I. Goldberg, P. Iyer, Z. Gross, *Chem. Eur. J.* **2002**, *8*, 2595.
- [11] a) Z. Gross, *J. Biol. Inorg. Chem.* **2001**, *6*, 733; b) S. Will, J. Lex, E. Vogel, H. Schmickler, J.-P. Gisselbrecht, C. Hauptmann, M. Bernard, M. Gross, *Angew. Chem.* **1997**, *109*, 367; *Angew. Chem. Int. Ed. Engl.* **1997**, *36*, 357.
- [12] Z. Gross, N. Galili, *Angew. Chem.* **1999**, *111*, 2536; *Angew. Chem. Int. Ed.* **1999**, *38*, 2366.
- [13] A. Mahammed, Z. Gross, *J. Inorg. Biochem.* **2002**, *88*, 305.
- [14] J. Bendix, I. J. Dmochowski, H. B. Gray, A. Mahammed, L. Simkhovich, Z. Gross, *Angew. Chem.* **2000**, *112*, 4214; *Angew. Chem. Int. Ed.* **2000**, *39*, 4048.
- [15] a) Z. Gross, L. Simkhovich, N. Galili, *Chem. Commun.* **1999**, 599; b) L. Simkhovich, Z. Gross, *Tetrahedron Lett.* **2001**, *42*, 8089; c) J. Grodkowski, P. Neta, E. Fujita, A. Mahammed, L. Simkhovich, Z. Gross, *J. Phys. Chem. A* **2002**, *106*, 4772; d) S. P. de Visser, F. Ogliaro, Z. Gross, S. Shaik, *Chem. Eur. J.* **2001**, *7*, 4954.
- [16] a) A. Mahammed, I. Goldberg, Z. Gross, *Org. Lett.* **2001**, *3*, 3443; b) I. Saltsman, A. Mahammed, I. Goldberg, M. Botoshansky, E. Tkachenko, Z. Gross, *J. Am. Chem. Soc.* **2002**, *124*, 7411.
- [17] D. Aviezer, S. Cotton, M. David, A. Segev, N. Khaselev, N. Galili, Z. Gross, A. Yayon, *Cancer Res.* **2000**, *60*, 2973.
- [18] F. Jerome, B. Billier, J.-M. Barbe, E. Espinosa, S. Dahaoui, C. Lecomte, R. Guillard, *Angew. Chem.* **2000**, *112*, 4217; *Angew. Chem. Int. Ed.* **2000**, *39*, 4051.
- [19] a) J. P. Morgan, C. Morrill, R. H. Grubbs, *Org. Lett.* **2002**, *4*, 67, and references therein. b) T. J. Seiders, D. W. Ward, R. H. Grubbs, *Org. Lett.* **2001**, *3*, 3225; c) T. Werle, G. Maas, *Adv. Synth. Catal.* **2001**, *343*, 37; d) T. Uchida, R. Irie, T. Katsuki, *Tetrahedron* **2000**, *56*, 3501; e) Y. Nishibayashi, I. Takei, S. Uemura, M. Hidai, *Organometallics* **1999**, *18*, 2291.
- [20] a) C. M. Che, J. S. Huang, F. W. Lee, *J. Am. Chem. Soc.* **2001**, *123*, 4119; b) G. Simonneaux, E. Galardon, C. Paul-Roth, *J. Organomet. Chem.* **2001**, *617*, 360; c) E. Galardon, P. Le Maux, G. Simonneaux, *Tetrahedron* **2000**, *56*, 615; d) Z. Gross, S. Ini, *Org. Lett.* **1999**, *1*, 2077, and references therein; e) Z. Gross, N. Galili, L. Simkhovich, *Tetrahedron Lett.* **1999**, *40*, 1571; f) Z. Gross, S. Ini, *Inorg. Chem.* **1999**, *38*, 1446.
- [21] T. Mlodnicka, B. R. James in *Metalloporphyrins Catalysed Oxidations*, (Eds.: F. Montanari, L. Casella), Kluwer Academic, Dordrecht, **1994**, pp. 121–148.
- [22] a) J. T. Groves, R. Quinn, *J. Am. Chem. Soc.* **1985**, *107*, 5790; b) J. T. Groves, K.-H. Ahn, R. Quinn, *J. Am. Chem. Soc.* **1988**, *110*, 4217.
- [23] J. T. Groves, M. Bonchio, T. Carofiglio, K. Shalyaev, *J. Am. Chem. Soc.* **1996**, *118*, 8961.
- [24] J. P. Collman, H. J. Arnold, *Acc. Chem. Res.* **1993**, *26*, 586.
- [25] L. Cheng, G. B. Richter-Addo in *The Porphyrin Handbook, Vol. 4* (Eds.: K. M. Kadish, K. M. Smith, R. Guillard), Academic Press, New York, **2000**, Chapter 33, Table 8, pp. 236–237.
- [26] K. M. Kadish, V. A. Adamian, E. V. Caemelbecke, Z. Tan, P. Taglatasta, P. Bianco, T. Boschi, G.-B. Yi, M. A. Khan, G. B. Richter-Addo, *Inorg. Chem.* **1996**, *35*, 1343.
- [27] M. Autret, S. Will, E. V. Caemelbecke, J. Lex, J.-P. Gisselbrecht, M. Gross, E. Vogel, K. M. Kadish, *J. Am. Chem. Soc.* **1994**, *116*, 9141.
- [28] J. P. Collman, C. E. Barnes, T. J. Collins, P. J. Brothers, *J. Am. Chem. Soc.* **1981**, *103*, 7030.
- [29] J. P. Collman, C. E. Barnes, P. N. Swepston, J. A. Ibers, *J. Am. Chem. Soc.* **1984**, *106*, 3500.
- [30] J. P. Collman, J. W. Proddollet, C. R. Leidner, *J. Am. Chem. Soc.* **1986**, *111*, 2916.
- [31] J. P. Collman, S. T. Harford, *Inorg. Chem.* **1998**, *37*, 4152.
- [32] M. J. Camenzind, B. R. James, D. Dolphin, *J. Chem. Soc. Chem. Commun.* **1986**, 1137.
- [33] a) Z. Xie, R. Bau, C. A. Reed, *Angew. Chem.* **1994**, *106*, 2566; *Angew. Chem. Int. Ed. Engl.* **1994**, *33*, 2433. b) W. R. Scheidt, C. A. Reed, *Inorg. Chem.* **1978**, *17*, 710.

Received: May 23, 2002 [F4120]